*Sensors and Materials*, Vol. 30, No. 3 (2018) 525–538
MYU Tokyo



S & M 1515

# Spatial and Seasonal Precipitation Variability in Eastern Fujian Based on Automatic Station Observation Data

Shiliang Zhang,[1] Tingcheng Chang,[1*] and Yuxia Wang[2]

[1]Department of Computer Science, Ningde Normal University, Fujian 352100, China
[2]Institute of Remote Sensing and Geographic Information Systems, Peking University, Beijing 100087, China

(Received November 7, 2017; accepted December 19, 2017)

***Keywords***: automatic station, precipitation, spatial pattern, seasonal distribution

The spatial and seasonal precipitation variability in eastern Fujian was studied using the monthly precipitation data from 1985–2014, the Mann–Kendall (M–K) statistical test method, the periodic test method, and the Pearson type III curve. The following conclusions were drawn: (1) There are obvious regional differences in the precipitation in eastern Fujian; more precipitation is found in the northern and western parts of eastern Fujian, while less precipitation is observed in the mid-eastern and western parts. In addition, Zherong Precipitation Center has the largest annual precipitation. (2) The precipitation in eastern Fujian fluctuates annually, but the variation is not significant, and the amount of precipitation is rather stable. The monthly precipitation shows bimodal characteristics, and the monthly distribution is uneven. (3) Strong precipitation in eastern Fujian mainly occurs from May to August, and the monthly difference in the frequency of strong precipitation in the north and mid-west is larger during the active period for strong precipitation, while the monthly difference between the eastern and western regions is smaller. The research results are important as a guide to the significance of the behavior of hydrological elements in eastern Fujian, to assist related departments in preventing mistake from floods, and to realize the sustainable utilization of water resources in the basin.

## 1. Introduction

The spatial and temporal distribution of precipitation is one of the key factors of local environmental change, which can in turn reflect regional environmental change in terms of spatial and temporal distribution of regional precipitation.(1) Many scholars have studied the characteristics of precipitation change in different regions of China, which is of great significance to the development of economic production. Yang *et al.* have studied the frequency of extreme precipitation as well as the temporal and spatial characteristics of precipitation in the Pearl River basin,(2) and found that the seasonal distribution of extreme precipitation has differences across the regions; Zhang *et al.* pointed out that the intensity of precipitation in the Pearl River basin is increasing,(3) the daily amount of precipitation is decreasing, and the frequency of occurrence of torrential rain is increasing. Chen *et al.* analyzed the characteristics

*Corresponding author: e-mail: 18250922163@163.com
http://dx.doi.org/10.18494/SAM.2018.1822

ISSN 0914-4935 

of temporal and spatial evolution of precipitation seasons in the East River valley,[4] and found that the precipitation in spring and winter is increasing, while it is declining in summer and autumn. Wang *et al.* found that the total precipitation in the Pearl River basin shows a slight increasing trend in the spring,[5] no significant increasing trend in the summer and winter, and no significant downward trend in the autumn. Zhang *et al.* determined that the annual precipitation in the upper reaches of the Zhujiang River is increasing; however,[6] the trend is not significant, and there is no obvious trend of change in spring, summer, autumn, and winter. Wu *et al.* found that, in spring and autumn after the 1980s in southern China,[7] studying a single feature index of precipitation trends, such as the intensity of precipitation, annual precipitation, or precipitation over four seasons, cannot completely reveal the changing environment of watershed precipitation in turns of evolving temporal and spatial characteristics. At present, the spatial and temporal characteristics of precipitation in the eastern Fujian area, especially the analysis of spatial distribution characteristics, are mainly for sites, so there is still a lack of combined space-time data on watershed precipitation, and especially a lack of detailed systems analysis for different areas at different times for watershed precipitation changes.[8] Therefore, this work analyzes the time variation characteristics of precipitation in different spatial areas and shows the spatial distribution characteristics of precipitation in the whole area of eastern Fujian. The paper is organized as follows: The second part describes the data. The third part introduces methodologies, including wavelet neural networks, the ant colony optimization algorithm, and the particle swarm optimization algorithm. A hybrid wavelet neural networks model is described in the fourth part. The fifth part describes applications and discussion of results. Conclusions are presented in the last part of the paper.

## 2. Regional Profiles and Data Sources

### 2.1 Data acquisition

This paper uses the data of monthly average precipitation from 1985–2014 in nine counties of eastern Fujian and uses this data as the average value for meteorological elements. The four seasons are divided into: spring from March to May, summer from June to August, autumn from September to November, winter from December to the following February.

The rainfall monitoring system fully integrates software and hardware resources and can realize all-weather remote automatic monitoring for the reservoir and record the dynamic change in the data from each meteorological station completely. The rainfall monitoring system consists of four parts: on-site testing equipment, remote monitoring equipment, a communication platform and a monitoring center. The four parts are described in the following.

On-site testing equipment consists of water level meters (such as ultrasonic water level meters, radar water level meters, and input water level meters), and rainfall meters and industrial cameras, responsible for measuring water level and rainfall data, and taking photos on site.

Remote monitoring equipment consists of a monitoring terminal (solar power supply type), responsible for collecting the data, and pictures taken by the field inspection equipment and transmitted as field information to the monitoring center through the general packet radio service (GPRS) network.

The communication platform includes the GPRS network and internet. The water level, rainfall data, and pictures are transmitted to the internet through the GPRS network and transmitted to the monitoring center server through the fixed IP address.

The monitoring center includes switches, servers, uninterruptible power supplies (UPSs), and other hardware and operating systems, databases, reservoir monitoring systems, and other software components. The topological structure of the data acquisition system is shown in Fig. 1.

## 2.2 On-site configuration of monitoring system

The rainfall monitoring system fully combines user demand and the on-site situation, using unique low power monitoring equipment, which not only saves equipment costs, but also reduces construction difficulties. We take the single measuring point as the example, as shown in Table 1. On-site installation system for automatic rainfall monitoring (Fig. 2) is installed all on land not involved in underwater operations.

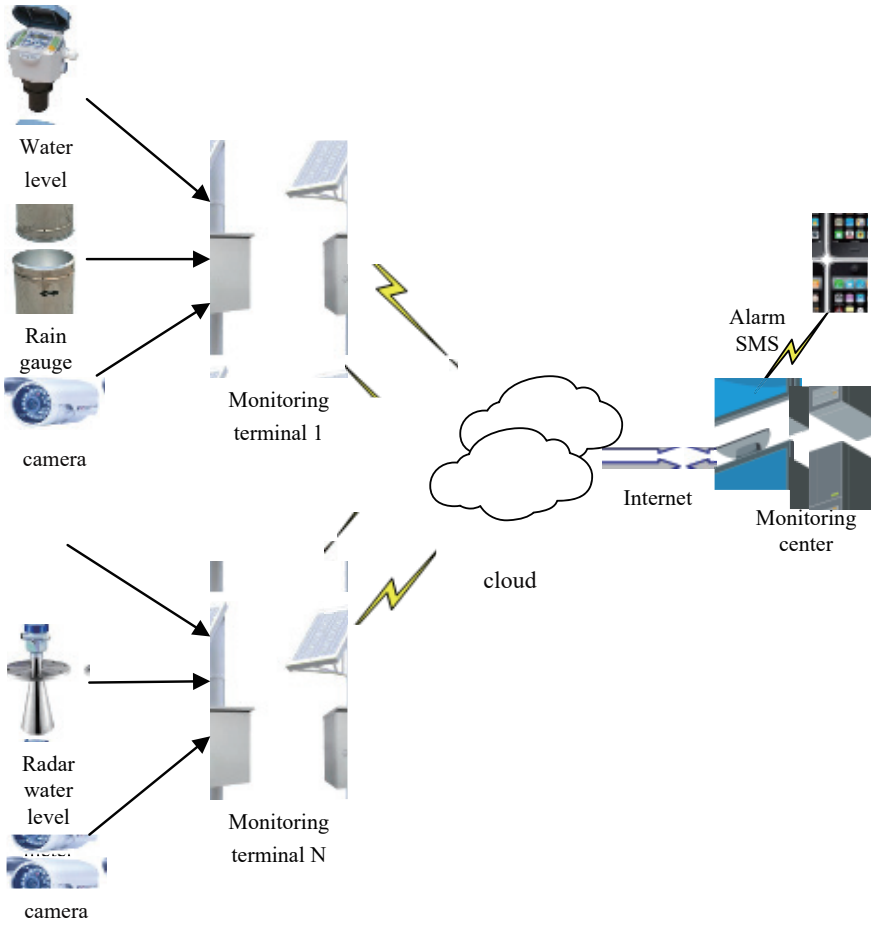


Fig. 1. (Color online) Topological structure of the data acquisition system.

Table 1
The monitoring equipment's configuration in the rainfall monitoring system.

| Equipment type | Equipment name | Equipment specifications | Quantity (set) |
|---|---|---|---|
| On-site testing equipment | Ultrasonic water level meter | 12 V DC power supply, 4–20 mA output | 1 |
| | Tipping bucket type rain gauge | Pulse signal output | 1 |
| | Industrial cameras | 5 V DC power supply, RS485 output | 1 |
| Remote monitoring equipment | Reservoir monitoring terminal | DATA-9201 | 1 |
| Solar power supply unit | Solar panel | 12 V/20 W | 1 |
| | Solar charge controller | 12 V/10 A | 1 |
| | Battery | 12 V/24 A | 1 |
| Other equipment | Equipment mounting rod and bracket | According to the environmental design for the site | 1 |
| | Lightning rod and grounding network | According to the environmental design for the site | 1 |
| | Installation of cables and auxiliary materials | | 1 |

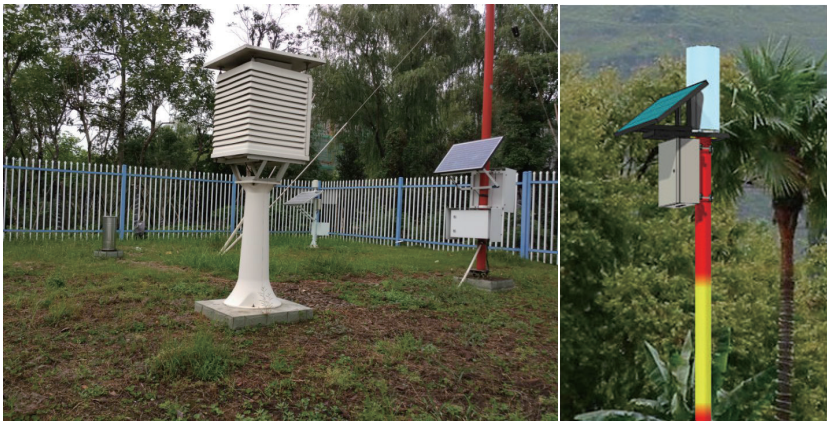

Fig. 2. (Color online) Automatic rainfall monitoring station.

## 3. Research Methods

### 3.1 Non-parametric Mann–Kendall (M–K) trend tests

The M–K nonparametric statistical test method recommended by the World Meteorological Organization is used in the trend analysis of the characteristic precipitation indices of each site.[9,10] A nonparametric testing method, also known as a distribution test, has the advantage of not requiring that the sample follow a certain distribution and is not distrusted by interference from a small number of abnormal values. It is suitable for analysis of data trends in hydrological meteorology and other non-normal data distributions. Assuming that climate change is stable, time series are independent of each other and maintain the same continuous distribution.[11] The M–K statistical method is as follows.

Define test statistics $S$:

$$S = \sum_{i=2}^{n} \sum_{j=1}^{i-1} sign(X_i - X_j), \tag{1}$$

where *sign* is a symbolic function. When $X_i - X_j$ is less than, equal to, or greater than zero, $sign(X_i - X_j)$ is respectively −1, 0, or 1. When the M–K statistical formula $S$ is greater than, equal to, or less than 0, respectively, we have:

$$\begin{cases} Z = (S-1)/\sqrt{n(n-1)(2n+5)/18}. & S > 0 \\ Z = 0. & S = 0 \\ Z = (S+1)/\sqrt{n(n-1)(2n+5)/18}. & S < 0 \end{cases} \tag{2}$$

When $Z$ is a positive value, it indicates an increasing trend; negative values indicate a decreasing trend. If the absolute value of $Z$ is greater than or equal to 1.28, 1.64, or 2.32, it goes through the 90, 95, or 99% reliability significance test, respectively.

### 3.2 Detection of sudden change by nonparametric M–K method

Suppose a time sequence is set up as follows: $x_2$, $x_3$, ..., $x_n$ constructs an order column $r_i$, $r_i$ representing a cumulative number of $x_i > x_j$ $(1 \leq j \leq i)$ samples. Then $S_k$ is defined as:

$$S_k = \sum_{i=1}^{k} r_i. \quad (k = 2, 3, ..., n) \tag{3}$$

In the equation, when $X_i > X_j$, $r_i = 1$; when $X_i \leq X_j$, $r_i = 0$ $(j = 1, 2, ..., i)$.

The mean $E(S_k)$ and variance $var(S_k)$ of the $S_k$ value are defined as:

$$E(S_k) = \frac{n(n+1)}{4}, \quad var(S_k) = \frac{n(n-1)(2n+5)}{72}. \tag{4}$$

Assuming the time series is stochastically independent, the statistics are defined as follows:

$$UF_k = \frac{S_k - E(S_k)}{\sqrt{var(S_k)}}. \quad (k = 1, 2, ..., n) \tag{5}$$

Among that, $UF_1 = 0$, $UF_k$ is a standard normal distribution, given a significance level $\alpha$. A normal distribution table obtains a critical value $U_\alpha$, when $|UF_k| > U_\alpha$, indicating that the sequence has a significant growth or reduction trend. All $UF_k$ will form a curve $c_1$, and using the reliability test we can see whether it has a trend or not. By referring this method to the inverse sequence, repeating the calculation, and multiplying the calculated value by −1, we can acquire $UB_k$. The term $UB_k$ is represented as $c_2$ in the graph. We then analyze the $UF_k$ and

$UB_k$ graphs. If the value is greater than 0, the sequence shows an upward trend; if less than 0, it indicates a downward trend. When the values exceed the reliability line, there is a significant upward or downward trend. If the intersection of $c_1$ and $c_2$ is located between the reliability lines, the point may be the beginning of a sudden change point.

Compared with other meteorological elements, due to the larger space-time scale of the variability of precipitation, the statistical significance of a change in trend is usually weaker, and the characteristic index of each precipitation will not show an obvious trend over a short time. Therefore, the standard for the trend test selected in this study is lower, that is, the test significance level is set to 0.05, 0.1, and 0.2 for corresponding confidence levels of 95, 90, and 80%. According to the degree of significance test, the variation trend of precipitation time at each site in the Pearl River basin can be divided into four kinds of situations: (1) the confidence level is less than 80%, which means there is no obvious trend; (2) the confidence level is between 80–90%, which means there is a weak trend; (3) the confidence level is between 90–95%, which means there is a stable trend; and (4) the confidence level exceeds 95%, which means there is a significant trend.

### 3.3 Cycle inspection method

In this study, wavelet analysis is used to examine the periodic variation of regional precipitation. This analysis is based on the Fourier transform, which can decompose a time series into the contributions of time and frequency. It is used to obtain the regulation of a complex time series. The evolutionary characteristics of the resolved time series are very effective in different scales. The wavelet analysis method is used to detect signal sudden changes, which can accurately determine the signal sudden change time.[12] This method is used to test the conclusions from the M–K method. There are many kinds of wavelet functions, based on the characteristics of the hydrological series, and we choose complex Morlet wavelets as small wave function,[13,14] the expression for which is:

$$\phi(x) = \sqrt{\pi f_b} e^{2\pi j f_c x} e^{\frac{x}{f_b}}, \tag{6}$$

where $f_b$ is the bandwidth parameter and $f_c$ is the center frequency of the wavelet.

### 3.4 Pearson type III frequency curve

The Pearson type III curve is introduced in this study to conduct hydrologic calculations. A Pearson type III curve has a small advantage in rainfall frequency analysis. The Pearson type III curve is an infinite asymmetric unimodal curve with a finite end at one end, and its realization principle is referred in the literature.[15,16] In a frequency calculation, the value $C_S$ is calculated for the sample, the $\varphi$ value table is checked to obtain the $\varphi_p$ values of different $p$ values, and then the estimated $E_x$,$C_v$ value is used. With the above-referenced formula, values can be calculated with various $p$ and corresponding $x_p$ values, so that the frequency curve can be drawn. Finally, the curve of frequency and empirical point-distance matching are used

to optimize the parameters by the method of fitting the frequency distribution curve and the sample empirical point distribution.

## 4. Analysis of Precipitation Distribution Characteristics

### 4.1 Average annual variation in precipitation and spatial distribution characteristics

#### 4.1.1 Cycle inspection method

The annual precipitation changes in eastern Fujian (LI_plot function) as shown in Fig. 3 show a slight upward trend. The highest precipitation year is 2006, when the annual cumulative value reaches 21109.1 mm, the lowest value is in 2003, when the cumulative value is only 10338.8 mm.

From Fig. 4, it can be seen that the main oscillation is described by the 5–7a during the 1984–2010-year evolution of precipitation is the vector addition of the oscillatory variation, which is then decomposed in the wavelet variance graph which strips out the primary cycle. There are four high-frequency centers and three other low-freqrency centers over this time scale; the years 1887, 1997, 2006, and 2014 have more rainfall centers, and the years 1993, 2003, and 2011 have fewer centers.

The modulus of Morlet wavelet coefficients is the reflection of the distribution of energy density in the time domain for different time scales; the larger the modulus of the coefficients, the stronger the periodicity of the corresponding period or scale. As can be seen from Fig. 5, in the process of precipitation evolution, the 10–13-year time scale modulus is the largest (greater than 2500), but the 1990–1995-year modulus is less than 500, indicating that, in this period of 10–13 years, the scale of the period of change is not obvious. After 1995, the modulus increases again, and the periodic changes of the 10–13-year time scale seems to be significant.

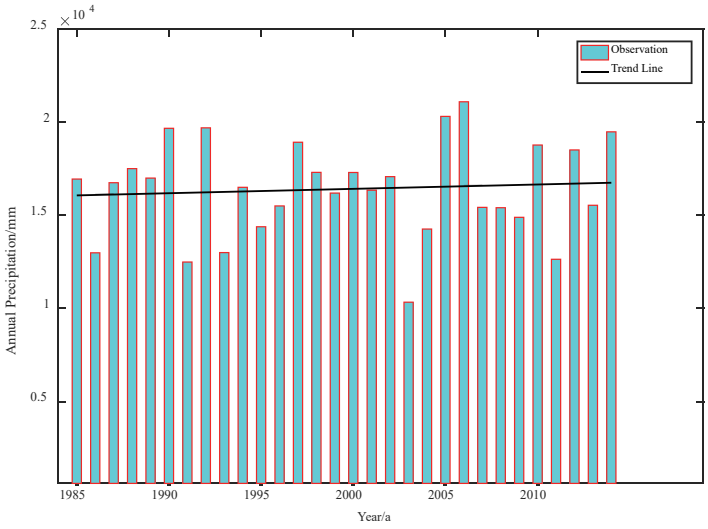


Fig. 3. (Color online) Annual precipitation changes.

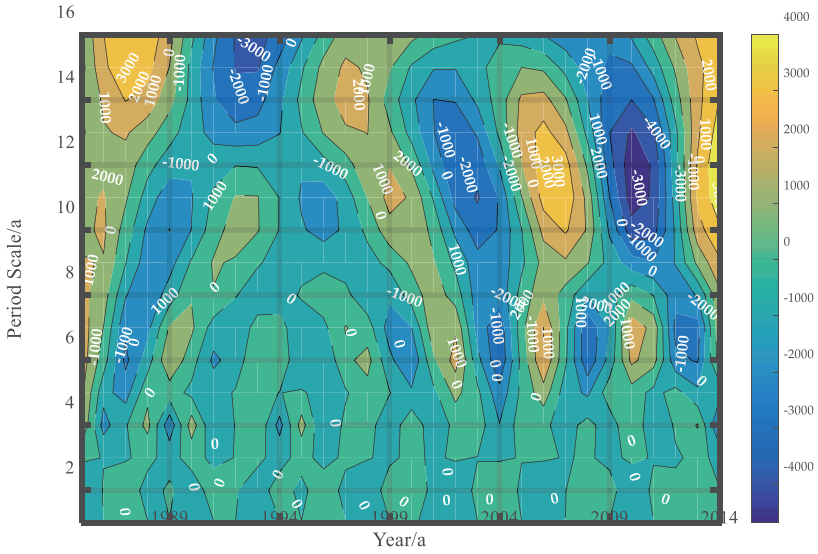


Fig. 4. (Color online) Contour lines for the real part of the precipitation wavelet coefficients.

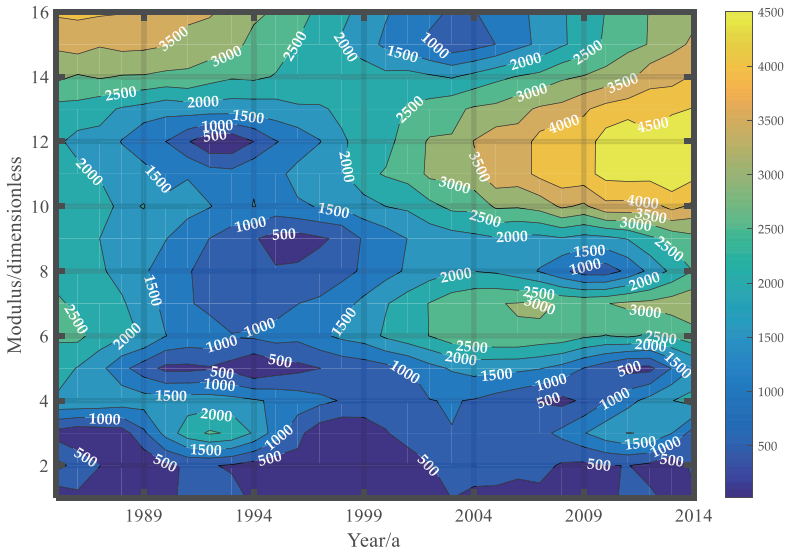


Fig. 5. (Color online) Contour map of wavelet coefficients modulus.

A wavelet variance graph can reflect the distribution of the fluctuation in energy with scale (a) in the precipitation time series. The graph can be used to determine the main period during the evolution of the precipitation. In the wavelet variance diagram (Fig. 6), there are 5 distinct peaks, which correspond to the time scales of 5a, 7a, 8a, 11a, and 15a in turn from small to large. Among them, the maximum peak value corresponds to the 11a time scale, indicating that the cyclic oscillation of about 11a (time scale) is the strongest as well as being the first main period of annual precipitation change. This shows that the fluctuation of the 5 cycles listed controls the variation of precipitation over the whole time domain. On the 11a feature time scale (Fig. 7), the average change period is about 5a, and the abundance-dry variation is approximately four cycles.

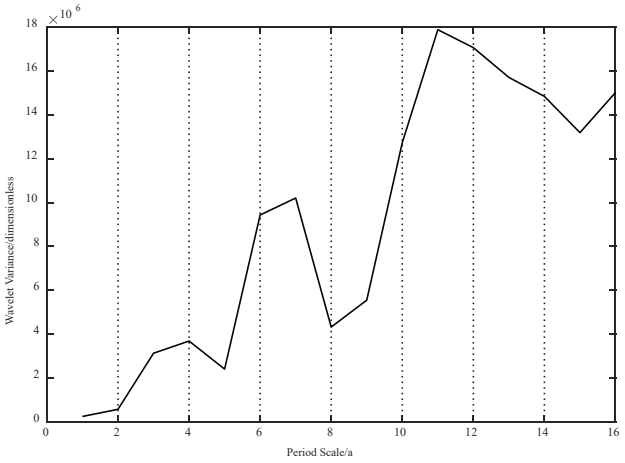


Fig. 6. Wavelet variance diagram.

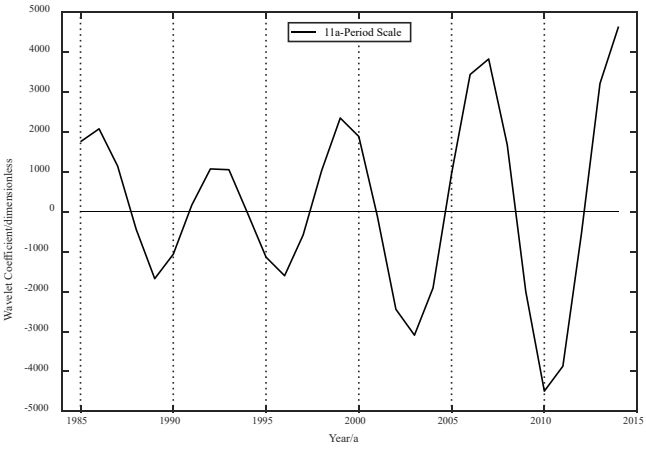


Fig. 7. Wavelet variance diagram of 11a feature time scale.

### 4.1.2 Analysis of the Pearson type III frequency curve method

Based on the analysis of precipitation frequency using the Pearson type III frequency curve in the eastern Fujian area in Fig. 8, the distribution regularity of annual precipitation in this area is basically in accordance with $E_X$ = 913.8 mm, $C_V$ = 0, and $C_S$ = 0. The Pearson type III frequency curve, thus the precipitation law in the area, annual precipitation in 21109.1 mm, and the above frequency is 5%, the annual precipitation is 14269.3 mm above the frequency is 80%. The corresponding frequencies in 25, 50, and 75% or more of annual precipitation were 17085.8, 16357.6, and 14899.7 mm, respectively.

### 4.1.3 Analysis by the M–K method

A k diagram is plotted, and in Fig. 9, the UF is a sequence of statistics calculated in positive chronological order. UB is the sequence of statistics calculated according to the reverse time sequence; from the UF curve, the rainfall in eastern Fujian shows an upward trend in the 1980s, and the rainfall fluctuation shows a decline after the 1990s. It tends to be more stable at the close of the 20th century. However, the overall change has always been within horizontal critical line with 0.05 significance. We conclude that rainfall will increase and reduce the change, which is not very significant, and the results of analysis and of the Pearson type III frequency curve analysis are basically consistent; rainfall changes are relatively moderate, extreme weather is less frequent. According to the point of intersection of UF and UB curves, it can be seen that, from 1952 to 2000, rainfall experienced many sudden changes. In the 1990s rainfall increase was a sudden change phenomenon; in 1990 and 2005 there were consecutive sudden changes, from 1990 to 1995 rainfall sudden changes were more frequent. Using M–K sudden change analysis, in 1990 and 1992 after the changes, through the years to 1997, there are no significant sudden changes. From 2005 to 2010, sudden changes occurred frequently, which may reflect that in recent years rainfall has changed greatly in eastern Fujian province, and the difficulty of prediction has increased.

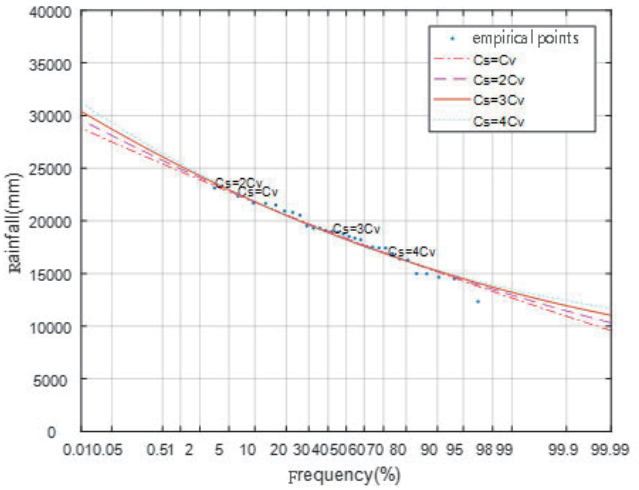


Fig. 8. (Color online) Theoretical frequency curves and empirical points according to the optimized graph.

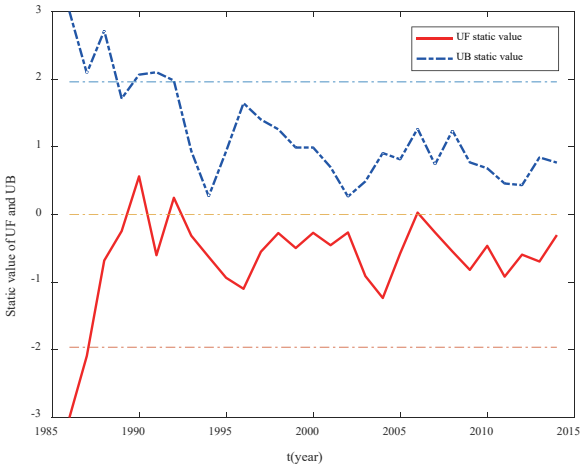


Fig. 9. (Color online) M–K chart.

### 4.1.4 ArcGIS interpolation analysis

Using ArcGIS10 geographic information software, the average annual precipitation distribution in nine counties of eastern Fujian Province was analyzed for the years 1985–2014 (Fig. 10). There were three counties and cities in eastern Fujian experiencing relatively strong precipitation, namely Zherong, Zhouning, and Jiaocheng, where the annual precipitation reached 2082.3, 2069.6, and 2020.3 mm, respectively. The area located in Zherong precipitation center has the largest annual precipitation, and it is one of the largest precipitation areas in Fujian, the center of rainstorms associated with typhoons. The annual precipitation in the counties and cities in Xiapu, Gutian, and Fu'an is smaller, where the yearly average precipitation is 1433.5, 1596.1, and 1627.9 mm, respectively. The area of smallest precipitation is in Xiapu, and unlike other coastal counties and cities (Jiaocheng, Fuding) as well as the mountainous gap, its precipitation does not reach 1500 mm. The precipitation is greater in the north and the mid-west, which is saddle-shaped, and less in the west and middle east. The distribution of precipitation in eastern Fujian is unstable, and the difference in precipitation between regions is obvious.

## 4.2 Analysis of the trends in seasonal precipitation

The average seasonal precipitation distribution (Fig. 11) in eastern Fujian in spring, summer, autumn and winter was obtained from monthly precipitation data; the average seasonal precipitation was the largest in summer. Since the 1980s, the precipitation in eastern Fujian has increased by an average of 182.3 mm, while the autumn average has decreased by 137.1 mm; in the early 21st Century (2001–2014), with the development of urbanization in the 1980s, vegetation has been somewhat damaged. From Table 2, it can be seen that precipitation in

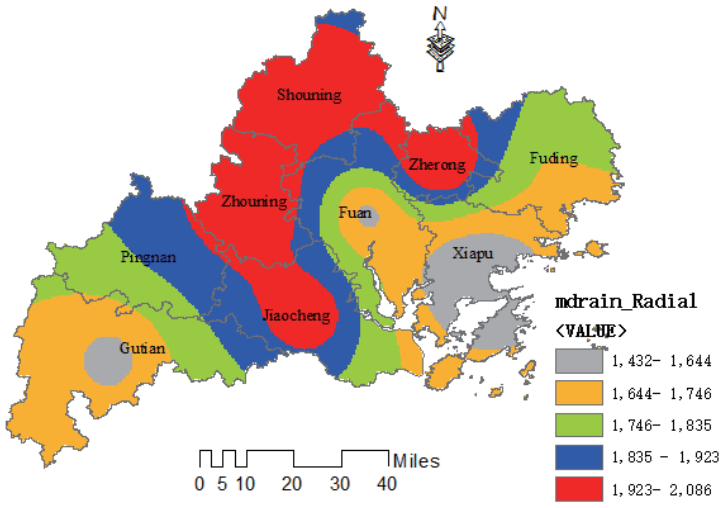


Fig. 10. (Color online) Annual precipitation distribution in the cities and counties of Fujian in 1985–2014.

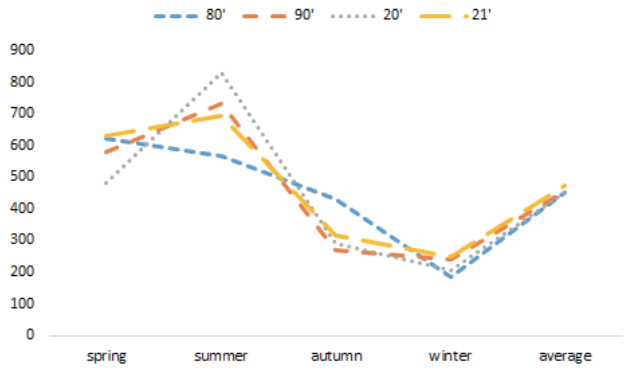


Fig. 11. (Color online) Seasonal precipitation distribution in eastern Fujian.

Table 2
Variation in water resources in different seasons (mm).

| Decade | Spring | Summer | Autumn | Winter | Average value |
|---|---|---|---|---|---|
| 80 | 621.4 | 568.9 | 429.5 | 185.3 | 451.3 |
| 90 | 578.9 | 731.3 | 270.2 | 239.2 | 454.9 |
| 20 | 482.8 | 828.7 | 289.6 | 204.9 | 451.5 |
| 21 | 629.1 | 693.9 | 317.2 | 248.4 | 472.2 |

Ningde is greater in spring and summer, accounting for 70.15% of the annual water resource, and it is the main source of precipitation. The precipitation in autumn and winter is lower, but the average precipitation has hardly changed.

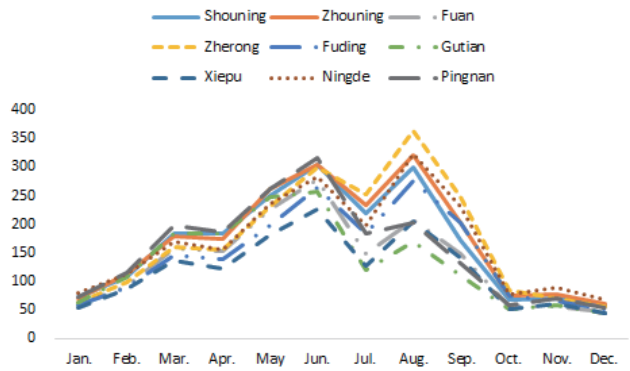


Fig. 12. (Color online) Monthly average precipitation in nine counties of the eastern Fujian.

### 4.3 Analysis of monthly average precipitation

According to the distribution of the average precipitation over many years (Fig. 12), it is known that the monthly precipitation may be described as a bimodal distribution: the precipitation in January to June increased monthly; the peak value fell in June, when the average precipitation reached 281.9 mm; a low value occurred again in July; precipitation in August reached the maximum value, when the average precipitation was 263.4 mm, which accounted for 29.9% of the total precipitation. Then the precipitation drastically reduced in December to January to a minimum of less than 66 mm. This change in the precipitation in eastern Fujian reflects the characteristics of the flood season and seasonal precipitation. From December to February, the winter has the least precipitation; March to June is the spring flood season, when precipitation gradually increased until June, when the precipitation reached the peak value; with the rainy season ending in late June, precipitation fell significantly in July; August is mainly affected by typhoons, and the precipitation increased; it was more than that in June, and reached a maximum value for the year; after September with the decrease of typhoon effect, the precipitation quickly fell back from October to November. Therefore, the amount of precipitation in the counties and cities in eastern Fujian was mainly determined by the rainy season from March to June and the typhoon season from July to September.

## 5. Conclusions and Discussion

Using linear regression, the M–K statistical test and the periodic test, this study analyzed the characteristics of rainfall in eastern Fujian. It reported the overall trend of rainfall, the level of abundance, and the rise and fall of rainfall in different time periods. The characteristics of precipitation are as follows:

(1) A rainfall change trend for the years 1985–2014 is not obvious. The first 20 years of rainfall has a slight upward trend; for more than 10 years in the middle, it is relatively stable. In recent years, it shows a weak downward trend, and the declining trend is relatively stable. The overall rainfall in many years has a slight downward trend. The characteristics of

large differences and uneven distributions of precipitation in Ningde reflect no significant climatic change. Since entering the 1980s, precipitation has fluctuated annually, but the variation is not significant, and the amount of precipitation is stable.

(2) The precipitation resources in eastern Fujian have obvious spatial-temporal distribution. The spatial distribution is characterized by the obvious regional differences of precipitation in eastern Fujian; the spatial distribution of precipitation in eastern Fujian is closely related to the topography, which is favorable for spring frontal precipitation and summer typhoon precipitation, which produces more abundant precipitation resources. The annual precipitation exceeds 1400 mm. The trend of annual precipitation in nine counties is the same, and the monthly precipitation appears bimodal. The precipitation difference across four seasons is obvious: autumn and winter precipitations are the lowest, spring and summer precipitations are the highest, and precipitation in June and August has peak values, which are closely related to the rainy season precipitation and to typhoons.

(3) Precipitation is mainly concentrated in March to September (except that there is less in July). Summer and spring precipitation is the main source of water resources in the eastern Fujian province. Affected by the terrain uplift, the northwest mountainous area easily forms the landform rain, rainfall in these place are obviously higher than that in the southeast coastal area. The annual average temperature is low in the mountainous region of northwest, and the evapotranspiration ability is weaker than that of the southeast coast. The distribution of evapotranspiration is the opposite of precipitation, that is, the availability of precipitation resources is higher in the northwest, and lower in the southeast.

There are many methods to study the characteristics of rainfall distribution. The M–K method and Pearson type III frequency curve method were analyzed in detail to understand the changes and the rainfall distribution characteristics. However, owing to the impact of rainfall factors, such as global climate, ecological environment, and others, it is possible to cause long term changes in rainfall, which are more obvious. These impacts require more scientific research and analysis.

## Acknowledgments

This work was supported by the Science and Technology Project of the Education Department of Fujian Province of China (No. JAT170652), the Project of Innovation Team of Ningde Normal University(No. 2017T05), the Science and Technology Project of the Ningde Bureau of Fujian Province of China (No. 20160065), and the Project of Ningde Normal University (No. 2016Z02). The authors appreciate the valuable comments and suggestions from the editors and reviewers.

## References

1 W. Qin, Q. Guo, C. Zuo, Z. Shan, and L. Ma: CATENA**147** (2016) 177.
2 T. Yang, Q. Shao, Z.-C. Hao, X. Chen, Z. Zhang, C.-Y. Xu, and L. Sun: J. Hydrol. **380** (2010) 386.
3 Q. Zhang, V. P. Singh, J. Peng, Y. D. Chen, and J. Li: J. Hydrol. **440** (2012) 113.
4 Y.-D. Chen, Q. Zhang, and X. X. Lu: Quat. Int. **244** (2011) 130.

5 W.-X. Lu, B.-J. Liu, and J.-F. Chen: J. Nat. Resour. **29** (2014) 80.
6 E. B. Łupikasza, S. Hänsel, and J. Matschullat: Int. J. Climatol. **31** (2011) 2249.
7 D.-J. Jiang, K. Wang, and Z. Li: Theor. Appl. Climatol. **104** (2011) 501.
8 T. Ye, Y.-P. Xu, and M. J. Booij: Theor. Appl. Climatol. **107** (2012) 201.
9 K. Ozgur and A. Murat: J. Hydrol. **513** (2014) 362.
10 G. Milan and T. Slavisa: Global Planet. Change. **100** (2013) 172.
11 T. B. Altın and B. Barak: Atmos. Res. **196** (2017) 182.
12 T. P. Le: Mech. Syst. Sig. Process. **95** (2017) 488.
13 K. C. Gryllias and I. A. Antoniadis: Mech. Syst. Sig. Process. **38** (2013) 78.
14 M. G. García and T. Koike: Spatial Statistics. **17** (2016) 50.
15 O. Kisi and M. Ay: J. Hydrol. **513** (2014) 362.
16 A. Asakereh, M. Soleymani, and M. J. Sheikhdavoodi: Sol. Energy **55** (2017) 342.